Supplementary Materials for

Fram Strait: Possible key to saving Arctic ice

Detelina Ivanova[1,*], Subarna Bhattacharyya[1], Leslie Field[2,4], Velimir Mlaker[1], Anthony Strawa[3],

Tim Player[2], Alexander Sholtz[2]

*Corresponding author. Email: detelina.ivanova@climformatics.com

This PDF file includes:

Supplementary Text:
- Arctic Dipole Anomaly
- List of Abbreviations

Figs. S1 to S9
Tables S1 to S2

Supplementary Text

Arctic Dipole Anomaly

There is no clear agreement about the Arctic Dipole Mode definition depending on the choice of dipole centers. Here we are referring to the Arctic Dipole Anomaly (ADA) *(15)* as the second empirical orthogonal function of monthly SLP north of 70^{o}N with one center in Kara/Laptev Seas and the other in the Canadian Archipelago extending through Greenland to the Nordic Seas. Using daily SLP anomalies *(16)* have derived a similar east-west dipole pattern centered in the Barents Sea and Greenland and Canadian Archipelago. Both studies found a significant correlation (e.g. 0.54 in *(16)*) between the SLP dipole anomalies and the sea ice export through the Fram Strait. Another known dipole pattern is the so-called “Barents Oscillation” *(30)* with SLP anomalies centers in the Barents Sea and Nordic Seas, which is rather active in the North Atlantic Sector of the Arctic and it is not relevant to our study.

List of Abbreviations:

ADA Arctic Dipole Anomaly

ANN Annual

AO Arctic Oscillation

BS Barents Sea

CAM Community Atmosphere Model

CESM Community Earth System Model

CICE Community Ice Code (Sea Ice Model)

CLM Community Land Model

DE Delta Eddington sea ice albedo model

FS Fram Strait

FSIE Fram Strait Ice Export

GHG Greenhouse gases

JAS July-August-September

JFM January-February-March

KS Kara Sea

NSIDC National Snow and Ice Data Center

PIOMAS Pan-Arctic Ice Ocean Modeling and Assimilation System

POP Parallel Ocean Program

TD Transpolar Drift

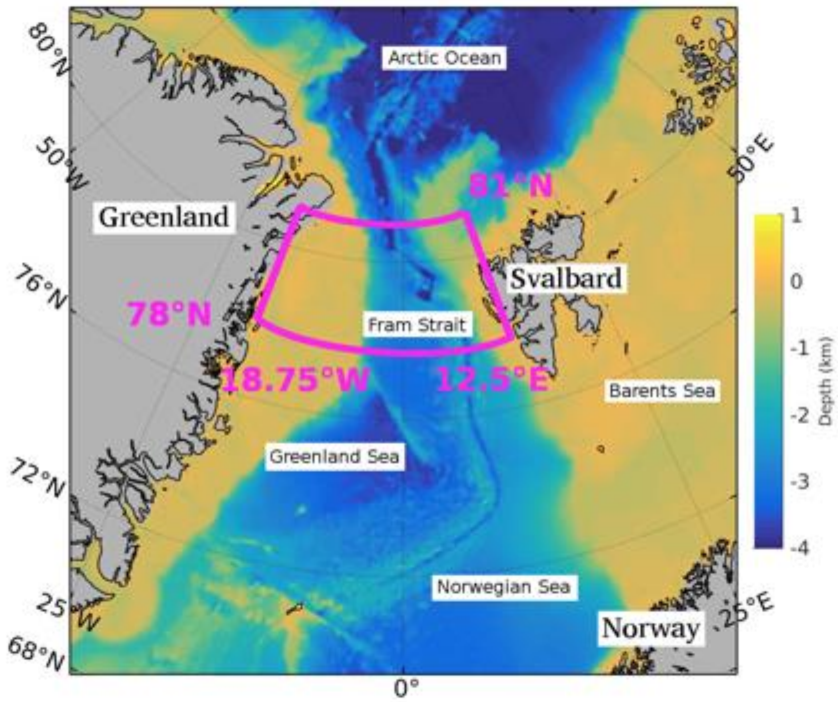

Fig. S1. Map of the Fram Strait region, outlined in magenta, with coordinates 78ºN-81ºN, 18.75ºW-12.5ºE and area of 151,200km2 , showing where the sea ice albedo is modified.

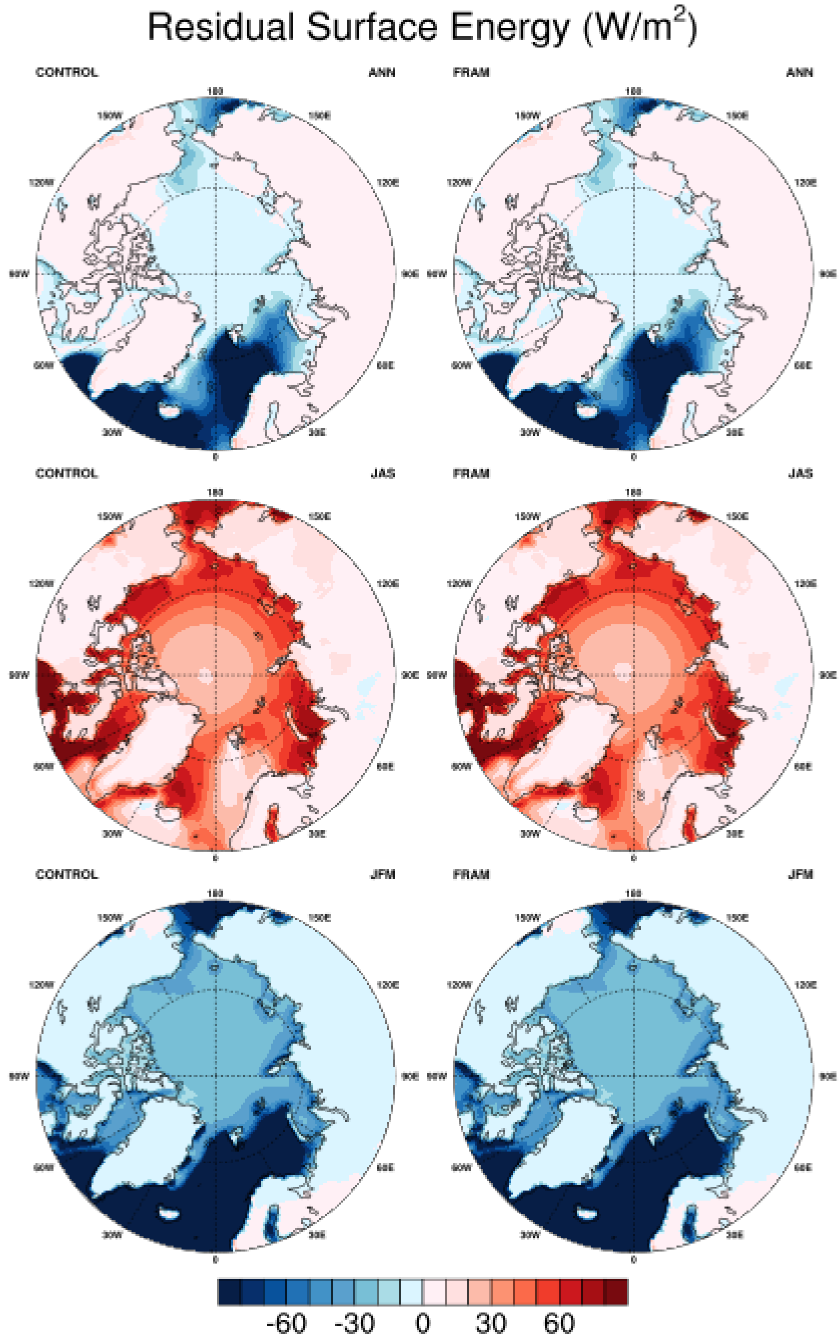

Fig. S2. Seasonal maps of the surface residual energy for CONTROL (left) and FRAM (right) ensemble mean climatologies (2001-2080). ANN - annual (top), JAS - July-August-September (middle) and JFM - January-February-March (bottom). Negative/Positive flux indicates loss/gain of heat.

Fig. S2 shows CONTROL and FRAM ensemble mean seasonal climatologies of the net radiation balance at the surface. The Arctic net radiation balance at the surface is predominantly negative (outgoing) with annual mean heat loss of -10W/m^2 (ANN). In the winter, the heat loss is -20W/m^2 in the interior of the basin to -30W/m^2 at the ice edge. During summer, the incoming solar radiation warms the surface, gaining heat of about 10W/m^2 at the North Pole to 40-70W/m^2 in the marginal seas. The differences between the FRAM and CONTROL case are mostly in the summer season (JAS) in the area of albedo perturbation in the Fram Strait (see Fig.2a and discussion in the main text).

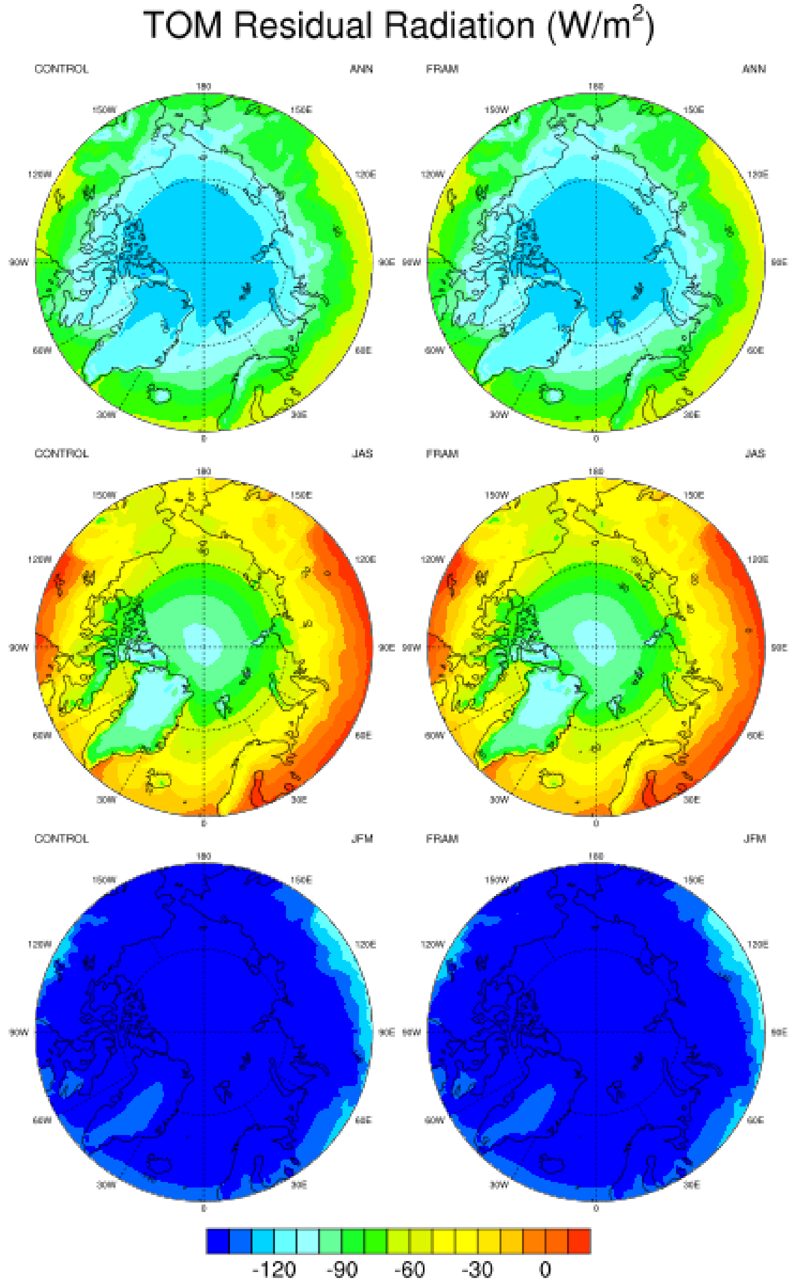

Fig. S3. Seasonal maps of the TOM residual energy: ANN (top), JAS (middle), JFM (bottom) for CONTROL (left) and FRAM (right) ensemble mean climatologies (2001-2080). Negative/Positive flux indicates loss/gain of heat.

Fig. S3 shows CONTROL and FRAM ensemble mean seasonal climatologies of the net radiation balance at the top of the model. At the top of the atmosphere (model) the net (residual) radiation flux in the Arctic is outgoing in open space, or losing heat and cooling, throughout the entire year. The heat loss in the winter (JFM) is more than -150W/m^2 basin wide, reducing in the summer (JAS) from -100W/m^2 in the central basin to -80W/m^2 at the 70ºN (including Fram Strait). The differences between the FRAM and CONTROL cases (see the main text) are mostly in the area of the Fram Strait region of albedo perturbation and also in the Barents and Kara Seas (Fig.2b in the main text).

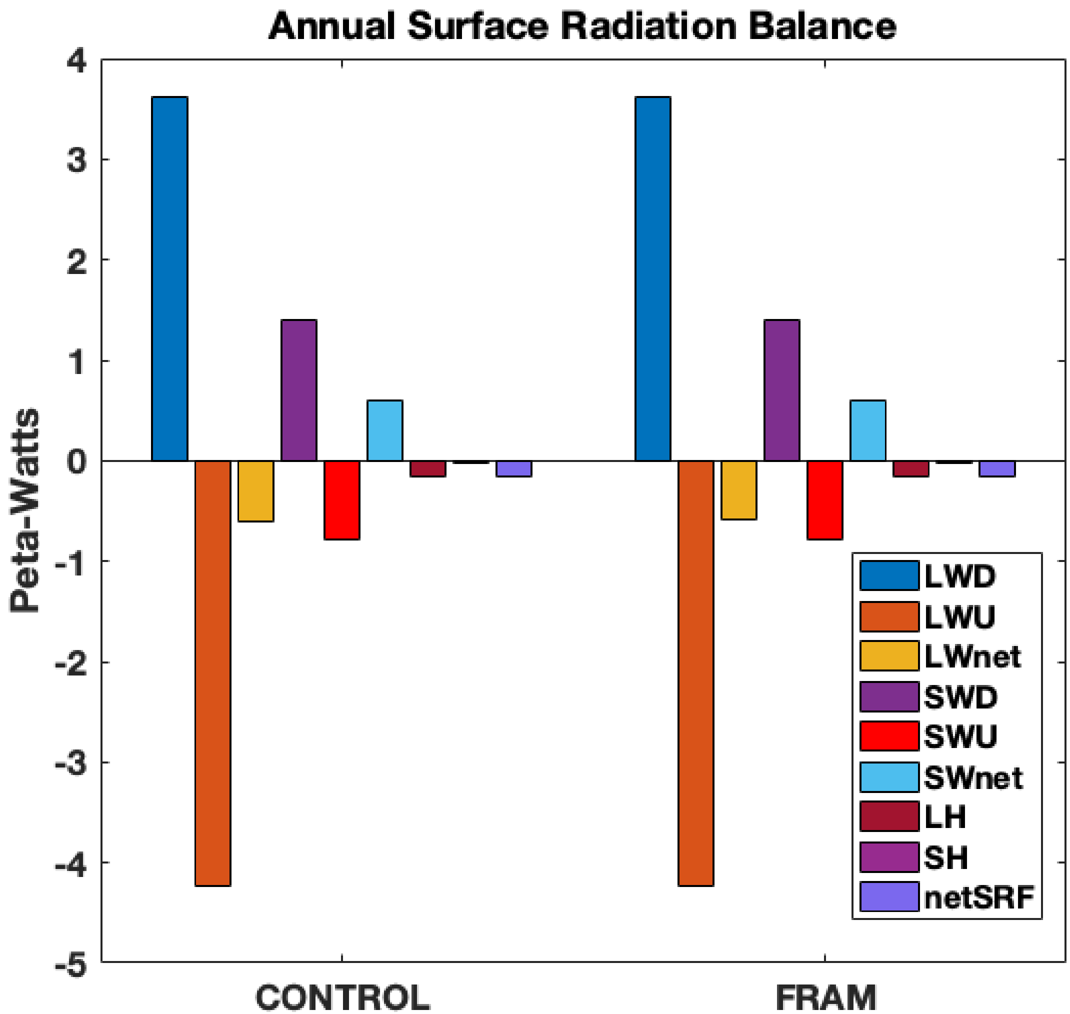

Fig. S4. Annual surface radiation balance components accumulated in the Arctic north of 70ºN: LWD - longwave down; LWU - longwave up; LWnet=LWU+LWD - net longwave radiation; SWD - shortwave down, SWU - shortwave up; SWnet=SWD+SWU - net shortwave radiation; LH - latent heat; SH - sensible heat; netSRF=SWnet+LWnet+LH+SH - residual surface energy. Positive direction is down. The values of the fluxes can be found in Table S1.

Fig. S4 (See also Table S1) shows the decomposition of the surface radiation balance in the Arctic. The budget components are accumulated north of 70ºN. The total incoming solar radiation at the Arctic ocean surface (shortwave down, SWD) in the CONTROL case is 1.3924 PW (Table S1). Part of it ~ -0.7862 PW is reflected (shortwave up, SWU) and the rest of 0.6062

PW (SWnet) is absorbed by the surface. In the albedo perturbation case (FRAM) with enhanced albedo in the Fram Strait region, the reflected shortwave flux (SWU) is increased with 4TW or with 0.5% compared to the CONTROL. This may not be significant when considering the entire Arctic radiation budget, but locally there are regions where these radiation changes are significant (Fig.2abc). The two longwave radiation components - longwave up (LWU) and longwave down (LWD) are the largest fluxes in the Arctic surface radiation balance with amounts of -4.2243 PW and 3.6255 PW correspondingly. They balance each other to a net longwave flux (LWnet) of -0.5988 PW outgoing from the surface in the CONTROL case (Table S1). The budget contributions of the turbulent heat fluxes are -0.1553 PW for the latent heat flux and -0.0188 PW for the sensible heat flux in the CONTROL case. With exception of the reflected shortwave flux all of the outgoing components (net longwave, latent and sensible heat fluxes) are reduced in the FRAM case most probably due to the reduced absorbed shortwave radiation (SWnet) and increased ice cover.

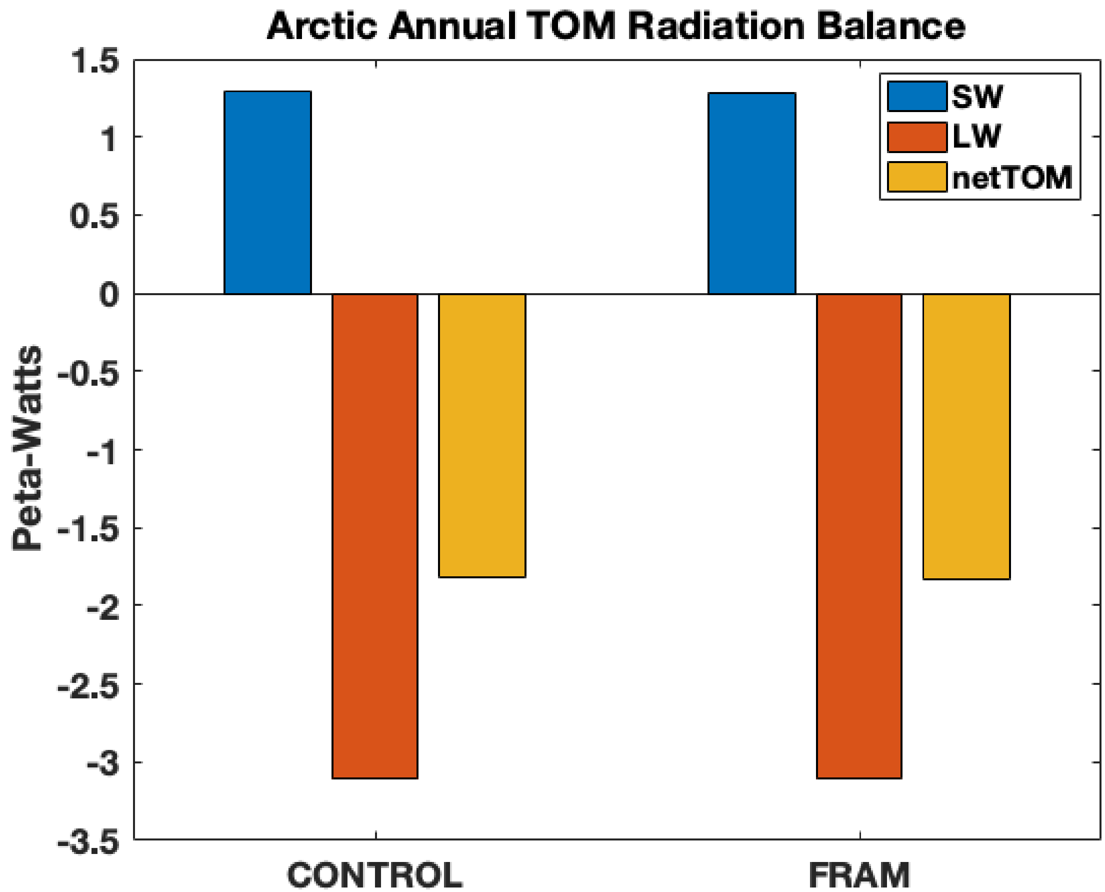

Fig.S5. Annual top of the model (TOM) radiation balance components integrated in the Arctic north of 70ºN: LW - net longwave radiation; SW - net shortwave radiation; netTOM=SW+LW - net radiation at TOM (negative is outgoing to space). The values of the fluxes can be found in Table S2.

Fig. S5 (see also Table S2) shows the Arctic radiation balance components integrated north of 70ºN at the top of the model. The balance here is formed by the net shortwave radiation flux (SW) of 1.2859 PW incoming to Earth and net longwave radiation (LW) of -3.1089 PW outgoing to open space, which results in net TOM radiation of -1.8230 PW outgoing to space in the CONTROL case. In the FRAM case the net shortwave radiation incoming to Earth is reduced with about 3.8 TW or 0.3% due to the increased albedo. There is a small reduction in the net longwave radiation 0.2 TW, but the overall net TOM radiation outgoing to open space is increased with 3.6 TW (0.2%) suggesting cooling of the Earth.

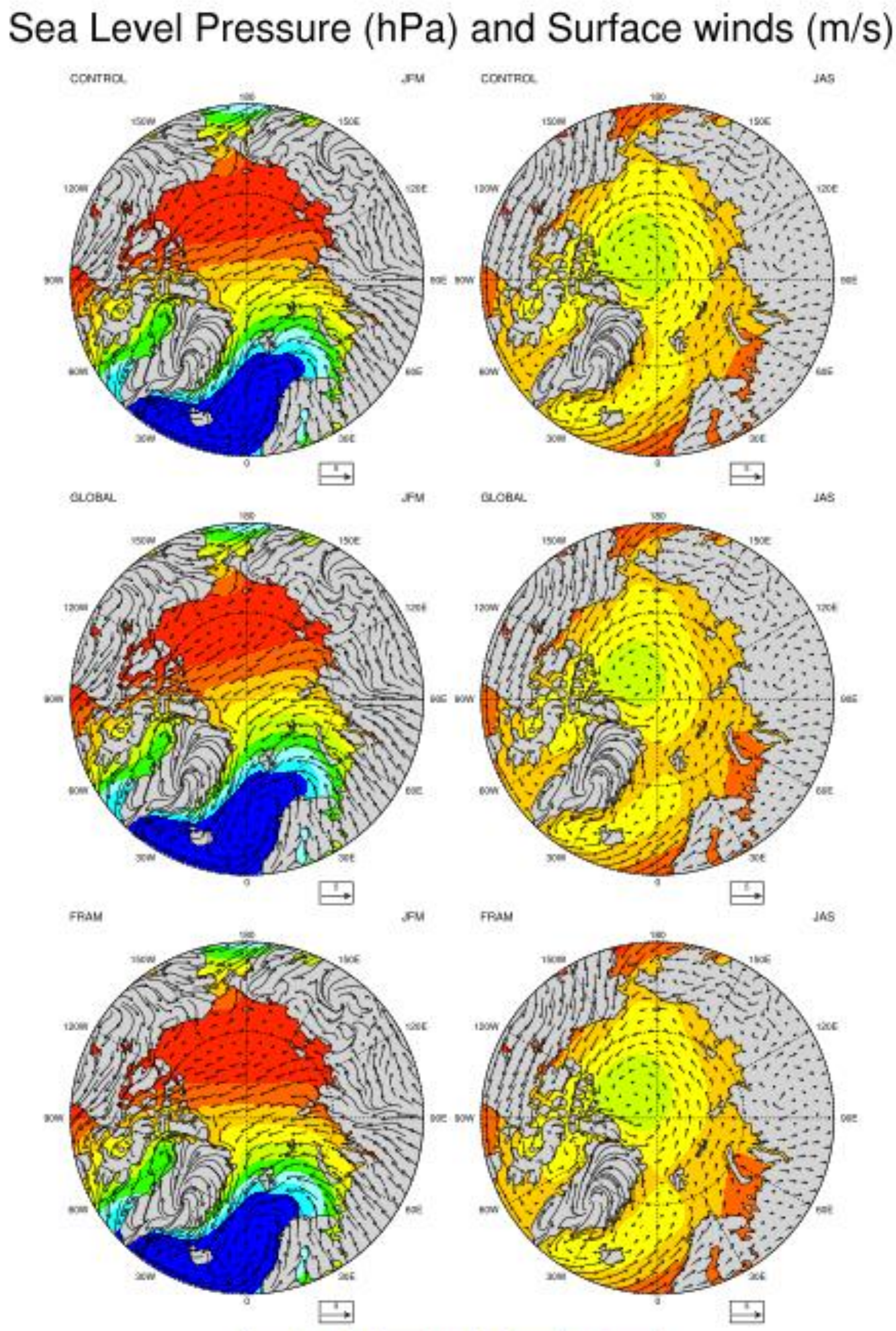

Fig.S6. Seasonal maps of sea level pressure (color) and surface winds (vectors): JFM (left) and JAS (right) in CONTROL (top), GLOBAL (middle) and FRAM (bottom) ensemble mean climatologies (2001-2080).

Fig. S6 shows CONTROL, GLOBAL and FRAM ensemble mean seasonal climatologies of the sea level pressure and surface winds in the Arctic. The dominant Arctic atmospheric pattern in the winter (JFM) consists of a high-pressure ridge stretching over the Beaufort Sea and East Siberian Shelf, and strong easterly winds flowing from Eurasia towards the Canadian Archipelago, turning southward around Greenland. These atmospheric dynamics transition in the late summer (JAS) to a basin-wide cyclonic system with low surface pressure center near the Canadian Archipelago and counter-clockwise divergent winds. The differences between the FRAM and CONTROL cases are shown in Fig.3 and discussed in the main text.

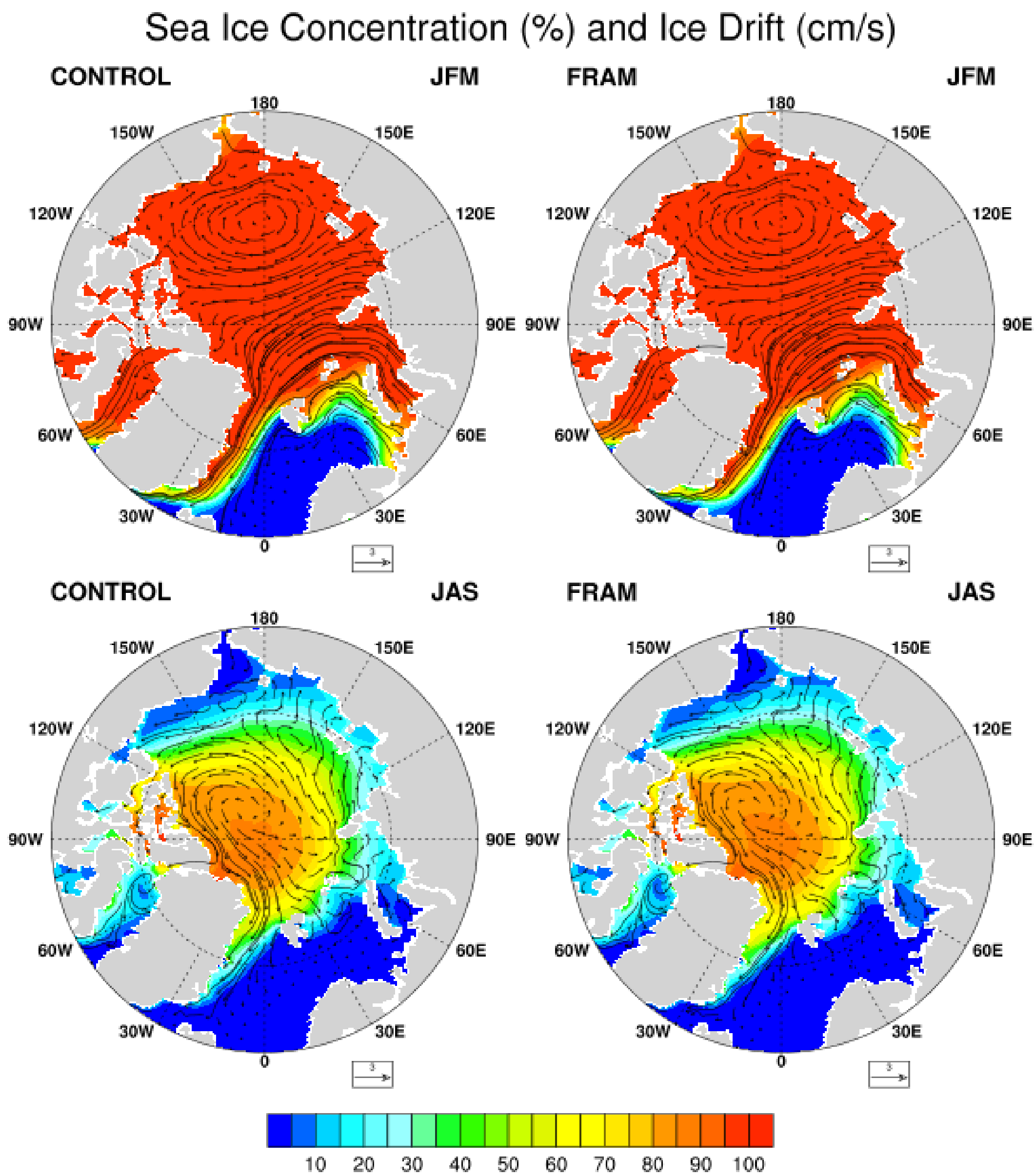

Fig.S7. Seasonal maps of the sea ice concentration (color) and sea ice drift (vectors): JFM (top), JAS (bottom) in CONTROL (left) and FRAM (right) ensemble mean climatologies (2001-2080).

Fig. S7 shows CONTROL and FRAM ensemble mean seasonal climatologies of sea ice concentration and sea ice drift in the Arctic. The winter (JFM) ice pack is with 100% ice concentration basin wide, drifted around the basin by a clockwise circulation of the Beaufort Gyre and the Transpolar drift moving ice from the Siberian shelf towards the Canadian archipelago and from Laptev and Kara Seas towards Fram Strait. In the summer (JAS), the ice pack is less compact with maximum ice concentrations of 90% in the Central Arctic rapidly reducing to 30-40% in the marginal seas. The sea ice drift is reversed compared to the winter, with anti-clockwise divergent circulation centered over the North Pole. The differences between the FRAM and CONTROL cases are discussed in the main text (See Fig.4a in the main text).

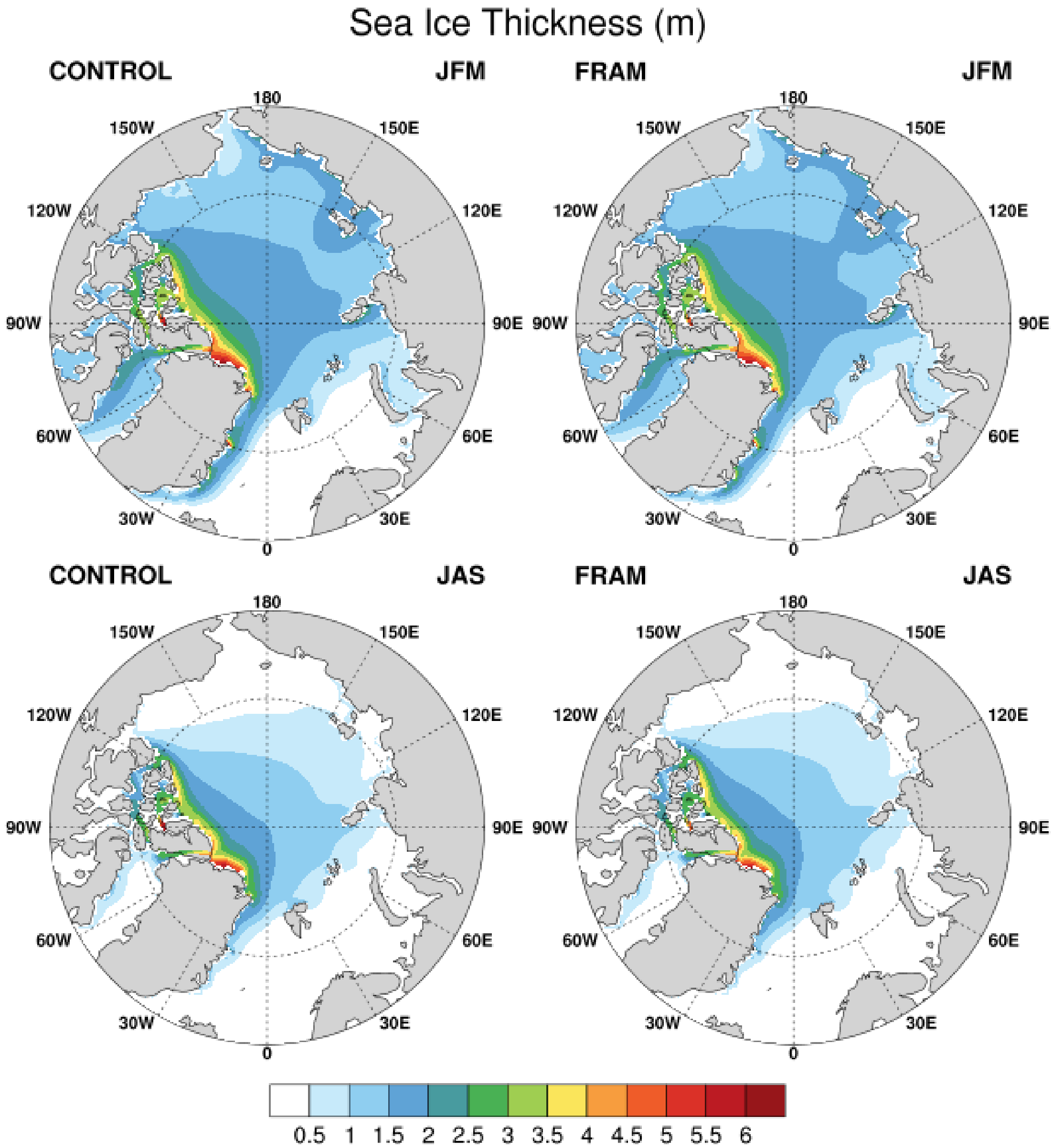

Fig.S8. Seasonal maps of sea ice thickness: JFM (top), JAS (bottom) in CONTROL (left) and FRAM (right) ensemble mean climatologies (2001-2080).

Fig. S8 shows CONTROL and FRAM ensemble mean seasonal climatologies of sea ice concentration and sea ice drift in the Arctic. The simulated thickness distribution is in good agreement with the ice thickness distribution observed in the 2000´s (See Kwok, 2018, Fig.1) with thickness of 1.5-2m at the North Pole, 1-1.5m in the Eastern Arctic, 0.5-1m in the Beaufort Sea. The thickest ice of about 4m is found along the northern coast of Greenland. The ice is thinning with half meter in the melt season. The differences between the FRAM and CONTROL cases are shown and discussed in the main text (See Fig.4b in the main text).

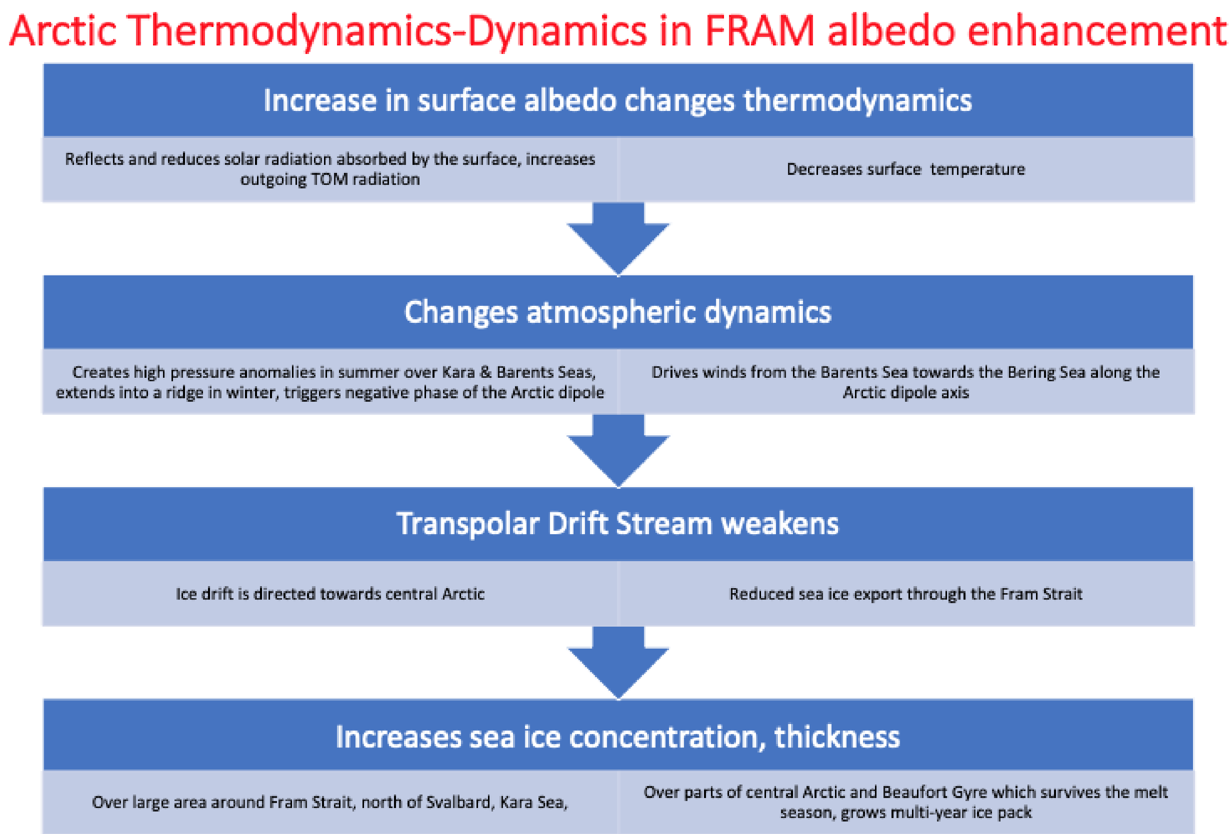

Fig. S9. Mechanisms Schematic

Mechanisms explaining the connection of the albedo (surface reflectivity) increase in Fram strait and strengthening the multi-year sea ice pack in the Arctic.

Increasing the sea ice albedo in the Fram Strait (FS) also increases the albedo in the Barents (BS) and Kara Seas (KS). These high albedo anomalies perturb the surface radiation balance there, reflecting more of the downwelling solar radiation and thus reducing the radiation absorbed by the surface in summer. This causes a cooling surface temperature anomaly which in turn creates a high surface pressure anomaly centered in the Barents and Kara Seas triggering a negative phase of the Arctic Dipole Anomaly. This drives the south-westerly winds from Barents and Kara Seas, along the Fram Strait towards the Beaufort Sea, forcing the sea ice to drift towards the central and western Arctic. The high-pressure anomaly extends and intensifies in winter into a high pressure ridge over the eastern Arctic with intensified winds directed towards Bering Strait. This atmospheric dynamic weakens the TD and the pressure gradient across the FS and consequently decreases the export of sea ice through FS (Fig.S9). Such changes in the large-scale sea ice circulation reinforce the multi-year sea ice growth near the Canadian Archipelago and central Arctic regions.

Table S1. Surface Radiation Balance. Longwave net=Longwave up +Longwave down; Shortwave net=Shortwave down + Shortwave up; Net surface radiation = Shortwave net + Longwave net + Latent Heat + Sensible Heat. Positive direction is down.

	CONTROL (PW)	FRAM (PW)	FRAM-CONTROL (PW)	FRAM-CONTROL (%)
Longwave down	3.6255	3.6263	0.0008	0.02
Longwave up	-4.2243	-4.2235	-0.0008	-0.02
Longwave net	-0.5988	-0.5972	-0.0016	-0.26
Shortwave down	1.3924	1.3922	-0.0003	-0.02
Shortwave up	-0.7862	-0.7902	0.0040	0.50
Shortwave net	0.6062	0.6020	-0.0042	-0.70
Latent Heat	-0.1553	-0.1550	-0.0003	-0.17
Sensible Heat	-0.0188	-0.0185	-0.0003	-1.12
Net surface radiation	-0.1666	-0.1688	0.0022	1.33

Table S2. Radiation balance at Top of the Model (TOM). Net TOM radiation = Shortwave net + Longwave net. Positive direction is down.

	CONTROL (PW)	FRAM (PW)	FRAM-CONTROL (PW)	FRAM-CONTROL (%)
Shortwave net	1.2859	1.2821	-0.0038	-0.30
Longwave net	-3.1089	-3.1087	-0.0002	-0.01
Net radiation	-1.8230	-1.8266	0.0036	0.20

Note: Positive fluxes are downwelling, negative are upwelling. The differences (FRAM-CONTROL) are taken from the absolute values of the fluxes i.e., positive differences are increases, and negative differences are decreases in FRAM case relative to the CONTROL case.